



Preparation, Characterization and Adsorption Capacity of Bauxite-Carbon Nanotube Composite

Suha Sahib Abd and Ahmed Mohammed Abbas[†]

Chemistry, College of Education for Pure Science Ibn-Al-Haitham, University of Baghdad, Baghdad, Iraq

[†]Corresponding author: Ahmed Mohammed Abbas

Nat. Env. & Poll. Tech.
Website: www.neptjournal.com

Received: 06-10-2018
Accepted: 04-02-2019

Key Words:

Bauxite clay
Bauxite-carbon nanotube
Adsorption
Methyl green dye

ABSTRACT

Iraqi bauxite clay was modified by using multiwall carbon nanotube (MWCNTs) as a modifying agent. The characterization of bauxite and bauxite/carbon nanotube was accomplished by using the Fourier transform infrared spectroscopy, scanning electron microscopy, atomic forces microscopy and X-Ray diffraction techniques. Uses the bauxite and bauxite/carbon nanotube composite for methyl green dye adsorption were achieved in a batch system. The adsorption equilibrium was attained at 60 and 45 min and adsorption efficiency reached maximum of 22 and 31% for bauxite and bauxite/carbon nanotube composite respectively, at an adsorbent dose of 0.01 g and initial dye concentration of 16 mg/L. Relying on the above shows that bauxite/carbon nanotube is a suitable adsorbent for the adsorption of methyl green dye, better than the bauxite clay.

INTRODUCTION

Raw clay consists of the main components, clay minerals, in which the platy structure has the predominance of the composition of these minerals. The individual layers in the clay structure can consist of two, three or four sheets either $(\text{AlO}_3(\text{OH})_3)_6$ octahedral or $(\text{SiO}_4)_4$ tetrahedral. These layers align themselves on each other with the van der Waal's gap between them to form interlayers. The interlayers are charged with a negative charge, which belong to the ionic groups that are compensated within the interlayers. The negative charge of the interstitial layers is equal to the positive ions between these layers. The positive ions between the interstitial layers can easily be replaced by other cations or molecules according to the desired chemical reaction. These cations Na^+ , Mg^{+2} , K^+ and Ca^{+2} are named ion exchange (Lee & Tiwari 2012). Nanoclay-composites are readily available, environmentally friendly, low cost, and many works of literature have accumulated on different perspectives of nanoclay-composite research over the past few decades. These include synthesis and characterization, surface properties, stability, manufacture of nanoclay-filled nanocomposite, and the use of nanoclays as precursors for the development of new materials (Ouellet-Plamondon et al. 2012).

Multi-wall carbon nanotubes (MWCNTs) are tubular with nanotube diameter and length from a few nanometers to a micrometer. MWCNTs consist of a two-dimensional graphene sheet wrapped more than once in a nanotube tube.

The world's first carbon nanotubes were first reported by Iijima (1991) as a result of the DC arc discharge of the graphite rod in an inert atmosphere of helium gas and carbon deposition on the cathode. Carbon nanotubes are likely to have applications in many areas of energy storage, sensors, sports equipment, actuators and electronics because of their unique structural, thermal, electrical and mechanical properties (Bellucci 2005). Carbon nanotubes have been widely used for pollutants adsorption from aqueous solutions. Numerous studies have been applied in the use of nanotubes as adsorbent for a number of heavy elements (Goering et al. 2008). Natural bentonite (B) has been modified by mixing with limited ratio of multiwall carbon nanotubes followed by high heat treatment in the inert atmosphere to form clay-nano composite material (BCA). It makes an adsorbent of rhodamine dye from wastewater. The nano composite adsorbent was characterized by XRD, SEM and FT-IR techniques. The effects of equilibrium time, adsorbent weight, pH and initial dye concentration on dye adsorption were studied. The nanocomposite sample BCA significantly enhances the adsorption of dye from aqueous solution, which indicates the possibility of using of BCA as a friendly adsorbent for adsorption of the dye from wastewater (Mohammed & Baytak 2016).

Two cheap materials (attapulgite and glucose) used for the preparation of clay-nano composite adsorbent by hydrothermal carbonization process under mild conditions. Compared to carbon-based materials, this clay-nano-composite exhibits a high adsorption capacity for Cr(VI)

and Pb(II) ions. The results show that this clay-nano-composite can be used as a low-cost, sustainable, and effective adsorbent for the adsorption of toxic heavy metals ions from water (Chen et al. 2011). The aim of the present work was to report the results of modification of bauxite by carbon nanotubes and the crystallographic structure of the bauxite/CNTs composites was confirmed by X-ray diffraction (XRD) measurements, while scanning electron microscopy (SEM) were used to characterize the morphology of the nano composite as well as the distribution of nanomaterials in the composite and investigate the adsorption capacity of (MG) dye onto bauxite and bauxite-composite.

MATERIALS AND METHODS

Materials

Carbon nanotube powder: The carbon nanotubes used in this work are of multi-walled type (MWCNTs), provided by ALDRICH. These were obtained by chemical vapour deposition (CVD) and contain 95% of the carbon nanotubes with an average diameter of 4.5 nm and length ranging from 1-1.8 μm .

Methyl green dye: Methyl green is a divalent cationic dye (name Basic Blue 20) that is chosen in this study as an adsorbate. Its molecular formula is $\text{C}_{26}\text{H}_{33}\text{N}_3\text{Cl}_2$ with molecular weight of 458.5 g/mol, as shown in Fig. 1. The stock solution of 100 mg/L of methyl green dye was prepared and λ_{max} was recorded by UV-visible spectrophotometer (Double beam, Shimadzu. 1800, Japan); it was found to be 618 nm.

Bauxite clay: The bauxite clay used in this work was supplied from the General Company for Geological Survey and Mining, Iraq, and obtained from Trifawi area in the western desert of Iraq. Analysis of bauxite has shown several compounds as given in Table 1 and expressed as oxides.

The clay of bauxite was obtained in the powder form. It was washed with an excess amount of distilled water to remove the soluble materials, then dried in an oven at 100°C for three hours and left to cool at 25°C, then saved in airtight containers. Using the sieve (200 mesh), the maximum particle size obtained was 75 μm . Therefore, this particle size was used in all the experiments throughout this work.

Preparation of Bauxite/Carbon Nanotubes Composite

The modified bauxite surface was achieved by suspension and diffusion of bauxite particles by the effect of ultrasound



Fig. 1: Chemical structure of methyl green dye.

(POWER SONIC405 Sonicater) in the ethanol solvent and then adding a certain amount of carbon nanotubes in two stages for two hours and then drying the lingering sediment in a laboratory oven at 80°C for 48 hours, and the dried substance sieved in order to get particle size of powder as 75 μm .

Characterization of Bauxite and Bauxite/MWCNTs Composite

Some of the characterization techniques were used for the identification of functional group (FT-IR); and the morphology and particle size designation (SEM, XRD, AFM) of bauxite before and after modification. Fourier transform infrared spectroscopy (FTIR) spectroscopic study of the sample was performed by Shimadzu Irtfinity-1(8400s). 0.5 g dried carbon sample was mixed with KBr (sample/KBr ratio was 1/100) and pressed into transparent thin pellet. A FTIR spectrum of carbon materials was obtained in the range of 4000 to 400 cm^{-1} . Spectral output was recorded by the transmittance as a function of wave number. Powder X-ray diffraction patterns of the prepared sample were taken by a X-ray powder diffractometer (X-ray Diffraction-6000 Shimadzu) using copper $k_{\alpha 1}$ of wavelength 1.54056×10^{-10} m. The scan was taken between 2θ of 5° and 2θ of 80° at increments of 0.02° with a count time of 4 seconds for each step. The samples were imaged on a scanning electron microscope (Tescan VEGA 3 SB) operated at 17 kV and observed the surface morphology at magnification of 25,000 times. For the AFM studies, bauxite particles were immobilized on an atomically flat mica surface (freshly cleaved) from a dilute suspension in ethanol. The sample was sonicated and allowed to sediment in a glass cylinder for 60 minutes. Some of the suspension from the glass cylinder (8 droplets) was put on the freshly cleaved mica square. The particles were dried by heating to 60°C for a few minutes in order to remove ethanol. AFM images were taken of samples at ambient conditions in air using a microscope (Atomic force microscopy- SPM AA3000USA2008).

Table 1: The chemical analysis of bauxite.

Compound	SiO ₂	Al ₂ O ₃	Fe ₂ O ₃	TiO ₂	CaO	MgO	SO ₃	L.O.I	Total
Wt %	15.7	64.2	0.9	1.3	1.5	0.1	0.3	16	100

Adsorption Experiments

An initially fixed concentration (16 mg/L) of the methyl green dye solution was shaken with (0.01 g) of each adsorbent at a specified temperature (25°C). The concentration of dye solution was determined spectrophotometrically at (5, 10, 15, 25, 35, 45, 60, 75, 90, 120, 150, 180) minutes. Equilibrium time is the time when the concentration remains constant.

The amount of (MG) dye adsorbed was determined from the initial and equilibrium concentrations and the volume of solution (Kannan & Veemaraj 2009).

$$q_e = \frac{V(C_o - C_e)}{m} \dots(1)$$

Where, q_e = the quantity adsorbed (mg), V = volume of solution (L), m = weight of adsorbent (g), C_o = initial concentration (mg/L), C_e = equilibrium concentration (mg/L).

RESULTS AND DISCUSSION

Fourier transfer infrared spectroscopy (FTIR): FTIR spectrum was used to identify the various silicon bonds in bauxite clay structure before and after modification. The FT-IR spectrum of bauxite (Fig. 2) shows several peaks where at 3622 cm^{-1} for the O-H stretch, at 3288 and 1637 cm^{-1} may be due to the presence of (H_2O) molecules from moisture. Si-O-Si bond is approved from 1053 cm^{-1} . The peak at 474 cm^{-1} refer to the presence of bonds such as Si-O-Mg or Si-O-Al, while the FT-IR of bauxite/MWCNTs composite (Fig. 3) shows changes in intensity and shape of peaks due to effects of carbon nanotube addition to bauxite clay (Abdullah et al. 2015, Shooto & Dikio 2012).

XRD analysis: The XRD spectrum of bauxite and bauxite/carbon nanotube composite is shown in Figs. 3 & 4 respectively. We observed from the Figs. 4 & 5 significant shift in most sites of the peaks of the X-ray diffraction spectrum of the modified bauxite surface by increasing the values of most of the diffraction angles (2θ) compared with the bauxite surface. On the other hand, we observe an increase in the distinctive peaks intensity in the confined area ($5 < 2\theta < 20$) while decreasing of peaks intensity for residual area of XRD spectrum of bauxite/carbon nanotube composite due to carbon nanotubes addition to bauxite surface; these lead to change in distance between crystalline levels. As a result of the pressure exerted by the carbon nanotubes on the structure of bauxite, due to the use of ultrasound in the process of modification, which led to the proliferation of large minutes of carbon nanotubes without affecting the proportion of crystallization (Dodoo-Arhin et al. 2013, Dikio 2011).

The AFM analysis: Atomic force microscopy (AFM) is a good identification instrument for surfaces materials at the

micro and nano level. The AFM measurements provide pictures (two and three dimensional) and granularity distribution charts for the bauxite and bauxite/carbon nanotube composite represented in Figs. 6 & 7. They show that the diameter of the particles is in the range of 156 nm to 74 nm for the bauxite and bauxite/carbon nanotube composite respectively. This indicates that lower average particle size obtained was for bauxite/carbon nanotube composite more than bauxite, which led to bauxite/carbon nanotube composite having the surface area and homogeneity more than bauxite clay (Zavala 2008).

Scanning electron microscopy (SEM): From SEM image (Figs. 8 & 9), we observe that the surface of the bauxite clay is not homogeneous, and its particles are large aggregation of different spherical sizes. So the bauxite particles have a surface area and radius equal to ($> 125 \mu m^2$, $> 6.3 \mu m$) respectively, while the modified bauxite surface with carbon nanotube shows high dispersion and the formation of smaller and more homogeneous aggregations so the modified bauxite particles have a surface area and radius equal to ($> 71 \mu m^2$, $> 4.7 \mu m$) respectively. These results are in agreement with AFM results (Yu et al. 2015).

Adsorption capacity: The adsorption capacity of bauxite and bauxite/carbon nanotube composite for methyl green dye versus the contact time is shown in Fig. 10. Adsorption quantity was increased with an increase in contact time that helps mineral bauxite to remove the largest amount of dye. Adsorption was very fast in beginning (in the first 5 min) for both bauxite and bauxite/carbon nanotube composite, and then it was increased slowly with time until reaching equilibrium. It was found that the equilibrium time was more than 60 and 45 min for both bauxite and bauxite/carbon nanotube composite respectively (Lin et al. 2007, Katal et al. 2012).

The efficiency for adsorption of (MG) dye (% Adsorption) was calculated as follows (Abbas et al. 2018):

$$Adsorption - percent = \frac{(C_o - C_t)}{C_o} \times 100 \dots(2)$$

Fig. 11 represents the comparison between the adsorption efficiency of bauxite and bauxite/carbon nanotube composite on methyl green dye. It indicates that the maximum dye adsorption is 32% and 22% at 0.01 g of bauxite/carbon nanotube composite and bauxite respectively.

CONCLUSION

It can be concluded that the modification process of bauxite with multi-walled carbon nanotubes did not alter the structural properties of bauxite, which was identified by different techniques (FT-IR, XRD, AFM, SEM), but the modi-

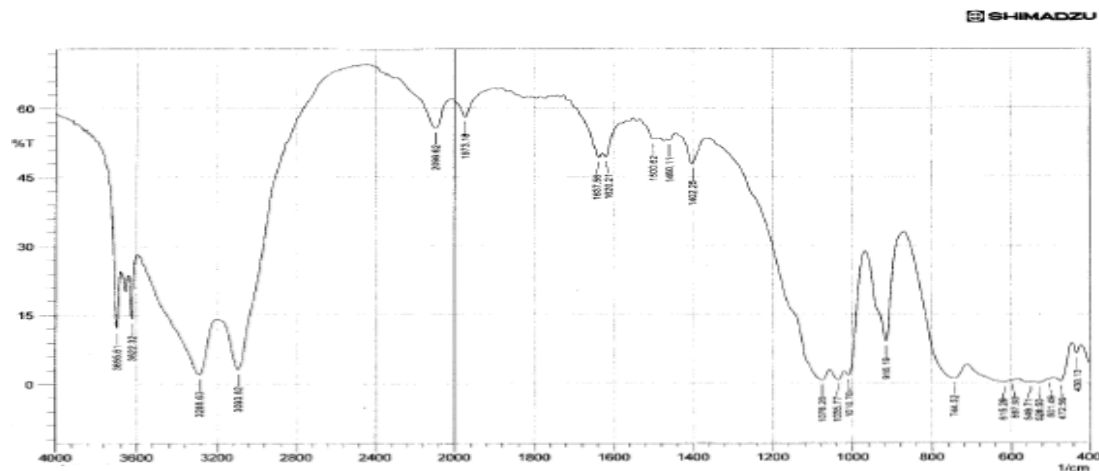


Fig. 2: FT-IR spectrum of bauxite clay.

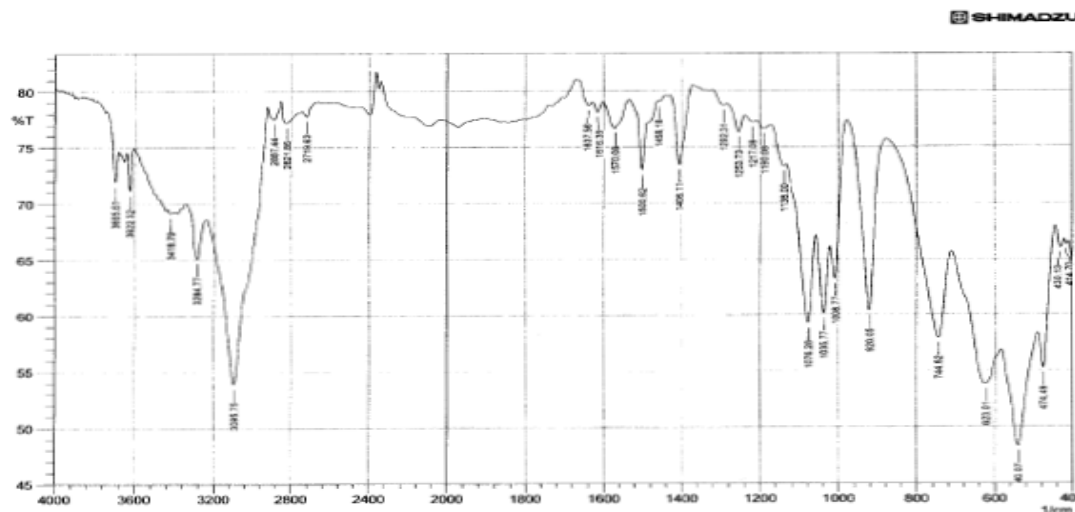


Fig. 3: FT-IR spectrum of bauxite/carbon nanotubes composite.

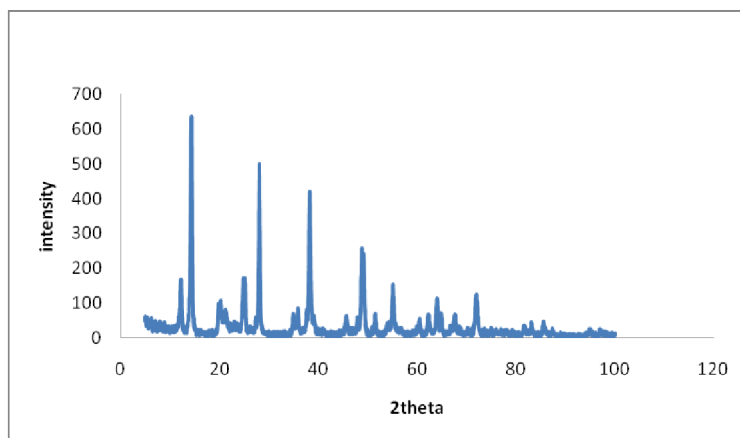


Fig. 4: XRD spectrum of bauxite clay.

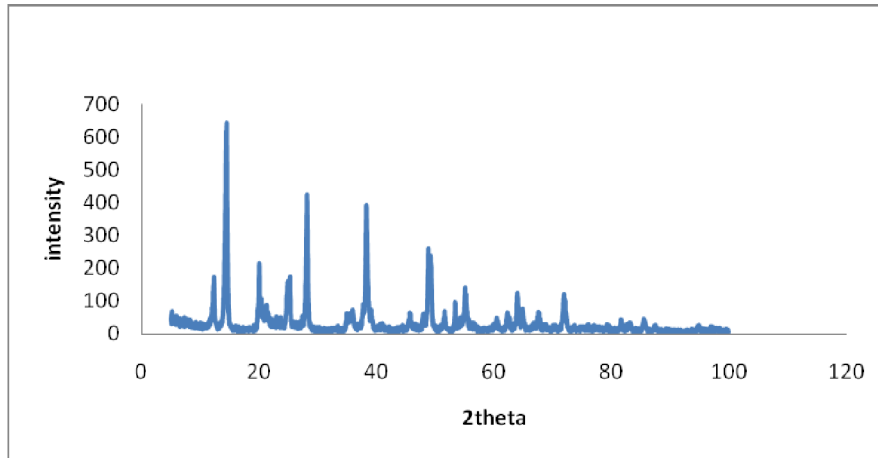


Fig. 5: XRD spectrum of bauxite/carbon nanotube composite.

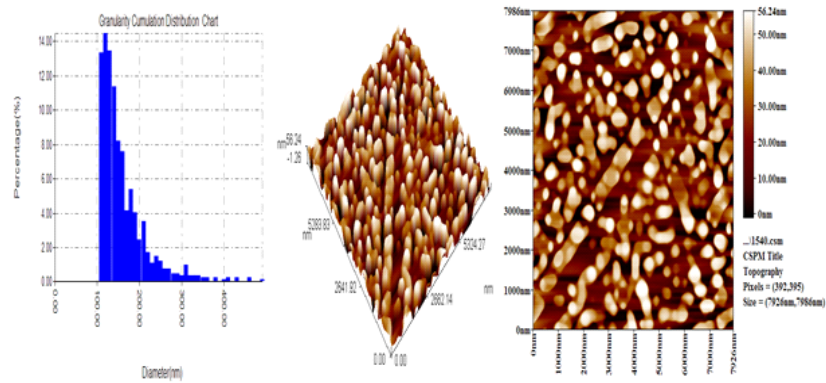


Fig. 6: AFM image for bauxite clay.

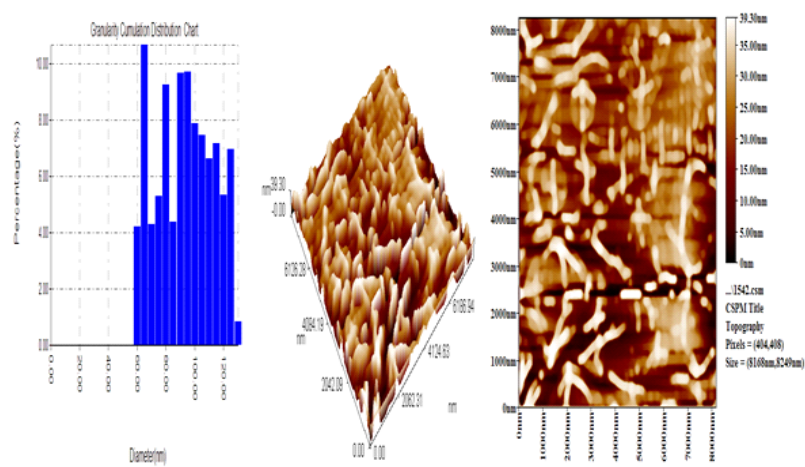


Fig. 7: AFM image for bauxite/carbon nanotube composite.

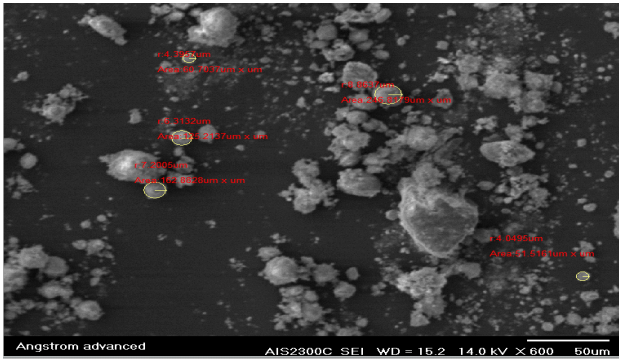


Fig. 8: SEM micrographs of bauxite.

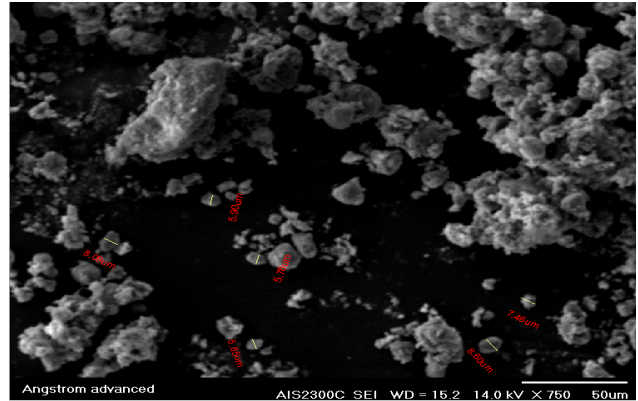


Fig. 9: SEM micrographs of bauxite/carbon nanotube composite.

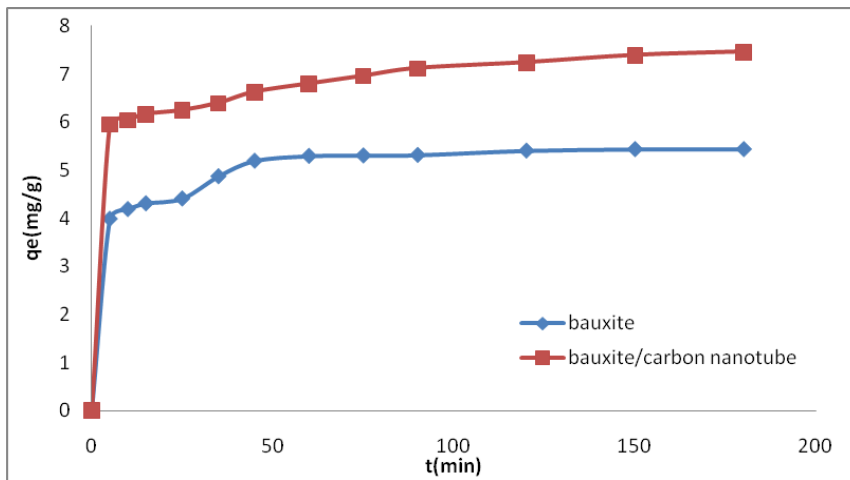


Fig.10: Effect of contact time on methyl green dye adsorption by bauxite and bauxite/carbon nanotube composite at 298 K.

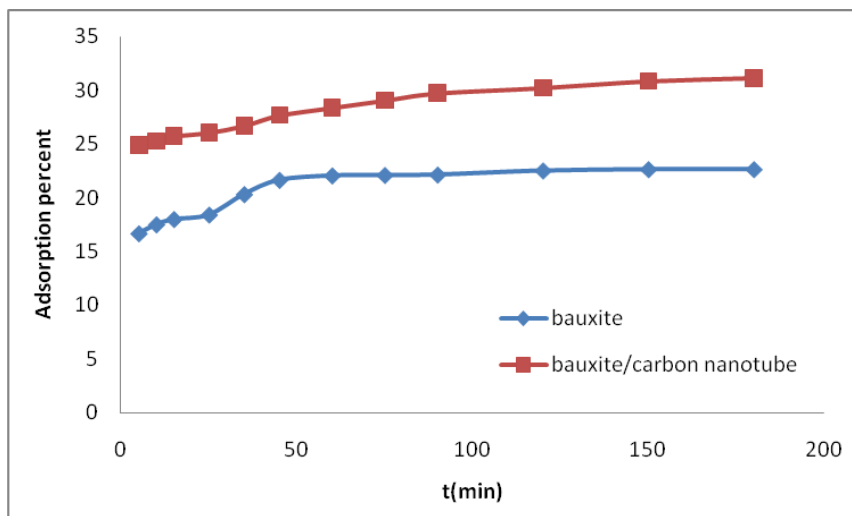


Fig. 11: Comparison between the adsorption efficiency of bauxite and bauxite/carbon nanotube composite.

fication process improved the properties of adsorption in bauxite. The maximum methyl green dye adsorption of bauxite/carbon nanotube composite was found to be 32%, whereas it was 22% for bauxite.

ACKNOWLEDGEMENTS

The authors thank the College of Education for Pure Science-Ibn Al Haithem/Baghdad University for their support to achieve this work.

REFERENCES

Abbas, A.M., Abdulrazzak, F.H. and Himdan, T.A. 2018. Kinetic study of adsorption of azo dye from aqueous solutions by zeolite and modified synthetic zeolite. *Journal of Materials and Environmental Sciences*, 9(9): 2652-2659.

Abdullah, M., Afzaal, M., Ismail, Z., Ahmad, A., Nazir, M. and Bhat, A. 2015. Comparative study on structural modification of *Ceiba pentandra* for oil sorption and palm oil mill effluent treatment. *Desalination and Water Treatment*, 54(11): 3044-3053.

Bellucci, S. 2005. Carbon nanotubes: Physics and applications. *Physica Status Solidi*, 2(1): 34-47.

Chen, L., Liang, H., Lu, Y., Cui, C. and Yu, S. 2011. Synthesis of an attapulgite clay@ carbon nanocomposite adsorbent by a hydrothermal carbonization process and their application in the removal of toxic metal ions from water. *Langmuir*, 27(14): 8998-9004.

Dikio, E. 2011. Morphological characterization of soot from the atmospheric combustion of kerosene. *Journal of Chemistry*, 8(3): 1068-1073.

Dodoo-Arhin, D., Konadu, D., Annan, E., Buabeng, F., Yaya, A. and Agyei-Tuffour, B. 2013. Fabrication and characterisation of Ghanaian bauxite red mud-clay composite bricks for construction applications. *American Journal of Materials Science*, 3(5): 110-119.

Goering, J., Kadossov, E. and Burghaus, U. 2008. Adsorption kinetics

of alcohols on single-wall carbon nanotubes: An ultra high vacuum surface chemistry study. *The Journal of Physical Chemistry C*, 112(27): 10114-10124.

Ijima, S. 1991. Helical microtubules of graphitic carbon. *Nature*, 354 (6348): 56.

Kannan, N. and Veemaraj, T. 2009. Removal of lead(II) ions by adsorption onto bamboo dust and commercial activated carbons - A comparative study. *Journal of Chemistry*, 6(1): 247-256.

Katal, R., Baei, M., Rahmati, H. and Esfandian, H. 2012. Kinetic, isotherm and thermodynamic study of nitrate adsorption from aqueous solution using modified rice husk. *Journal of Industrial and Engineering Chemistry*, 18(1): 295-302.

Lee, S. and Tiwari, D. 2012. Organo and inorgano-organo-modified clays in the remediation of aqueous solutions: an overview. *Applied Clay Science*, 59-60: 84-102.

Lin, J., Zhan, S., Fang, M. and Qian, X. 2007. The adsorption of dyes from aqueous solution using diatomite. *Journal of Porous Materials*, 14(4): 449-455.

Mohammed, M. and Baytak, S. 2016. Synthesis of bentonite-carbon nanotube nanocomposite and its adsorption of rhodamine dye from water. *Arabian Journal for Science and Engineering*, 41(12): 4775-4785.

Ouellet-Plamondon, C., Lynch, R. and Al-Tabbaa, A. 2012. Comparison between granular pillared, organo-and inorgano-organo-bentonites for hydrocarbon and metal ion adsorption. *Applied Clay Science*, 67: 91-98.

Shooto, N. and Dikio, E. 2012. Synthesis and characterization of diesel, kerosene and candle wax soot's. *Int. J. Electrochem. Sci.*, 7: 4335-4344.

Yu, F., Deng, H., Bai, H., Zhang, Q., Wang, K. and Chen, F. 2015. Confine clay in an alternating multi layered structure through injection molding: A simple and efficient route to improve barrier performance of polymeric materials. *ACS Applied Materials & Interfaces*, 7(19): 10178-10189.

Zavala, G. 2008. Atomic force microscopy, a tool for characterization, synthesis and chemical processes. *Colloid and Polymer Science*, 286(1): 85-95.